scientific reports

OPEN

Higher order chemical reaction effects on Cu−H₂O nanofluid flow over a vertical plate

Padmaja K & Rushi Kumar B✉

Many fluids used in industries will possess a uniform velocity acting along with it. Although a few researchers have analyzed the fluid flow along with a constant velocity but such modeling in nanofluids is quite new. The novelty of this work is the numerical evaluation of a nanofluid with a constant velocity through a vertical plate in a porous medium under Dufour as well as Soret impacts coupled with a higher order chemical reaction. A rotating MHD nanofluid is investigated for both heat as well as mass transfer. An incompressible, steady-state fluid is subjected to flow through a semi-infinite plate by taking into account viscous dissipation as well as a magnetic field. Flow equations are typically represented by PDEs that are nonlinear and coupled. The PDEs are changed to ODEs by similarity transformation variables. Runge-Kutta method of 4th order accuracy along with shooting technique is employed to solve the converted system of ODEs. Cu−H₂O is used to provide an in-depth analysis of the examined problem. In order to account for practical considerations, the maximum order of the chemical reaction is limited to 3 and a comparative analysis is provided for 1st and 3rd order chemical reactions. For different physical quantities, different numerical values that are obtained using MATLAB are used to analyze various properties regarding the flow. Heat transfer, and mass transfer rates are discussed using graphs and tables. Compared to low order chemical reactions, high order chemical reactions allow higher rates at which the reaction takes place, thus allowing greater rates of heat and mass transfer.

There is a wide range of applications for heat, and mass transfer with higher order chemical reactions through porous media in chemical and water industries. Industrial processes like filtration, distillation, cooling, and drying rely on heat, and mass transfer, in conjunction with chemical reactions. In industries, the rate at which a process occurs is extremely essential; the faster the rate, the lesser time is required in the process, which in turn reduces the amount of time required for storage, resulting in a process that is more efficient and comparatively affordable. The order of a chemical reaction explains the relationship between the concentration of a species and the rate at which the reaction takes place. A reaction is of nth order if the rate of a reaction is directly proportional to the nth power of concentration of the species. Chemical reactions occur at a faster rate as the order of the reaction increases. It is necessary to have faster rates of chemical reaction in order to manufacture chemicals such as fertilizers, polymers, and color dyes on a large scale. The effects of higher order chemical reactions in porous media have previously been studied by Rahman et al.[1], Mallikarjuna et al.[2], Rajani et al.[3], Matta et al.[4] and Sastry et al.[5].

Thermal energy is used extensively in industrial operations including expulsion, papermaking, and cooling computer chips to generate finished products with desired qualities. A significant role for viscous dissipation, and joule heating is to modify temperatures by acting as an energy source. Heat transfer rates change when temperatures do. Several authors Chen[6], Alam et al.[7], Jaber[8], Pandey and Kumar[9], Prakash et al.[10], Reddy et al.[11] have researched this topic extensively.

By passing a fluid through the product, heat can be either transferred away from or transferred towards the product. There must be ways of transferring heat efficiently without wasting significant energy. Some metals, which have high thermal conductivity, can be combined with a liquid, such as water, to transfer heat efficiently. In their research, Choi and Eastman[12] used nanometer-sized particles and a base fluid to develop nanofluids, which are colloidal suspensions containing nanometer-sized particles. As a result of its high compatibility, this fluid is capable of inducing or reducing heat transfer. The study of nanofluids to enhance the rates of heat transfer in solar thermal applications has been done by Sheikholeslami[13–15].

Department of Mathematics, School of Advanced Sciences, VIT, Vellore, Tamil Nadu 632014, India. ✉email: rushikumar@vit.ac.in
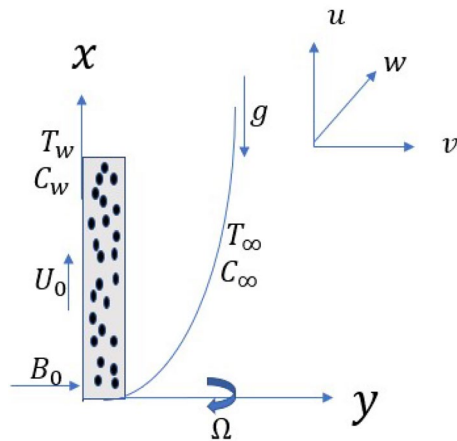
Figure 1. Flow geometry.

In their study, Jagadha et al.[16] conducted an investigation on the flow of nanofluid over porous vertical plate taking into account factors like dispersion, radiation, dissipation, chemical reaction, as well as Brownian motion, and some dimensionless number effects. Swain et al.[17] made an analysis of the effect of viscous dissipation, joule heating, magnetic parameter, and suction parameter on the MHD flow of a nanofluid with a higher order chemical reaction. This study was conducted through a stretching surface in a permeable medium.

In an analytical study, Alaidrous and Eid[18] examined how nanofluid moves through a porous stretching sheet by considering the impacts of higher order chemical reaction, radiation, Joule heating, and viscous dissipation. Gopal et al.[19] investigated numerically how an MHD nanofluid flow in a porous stretching sheet is affected by the impacts of higher order chemical reaction as well as viscous dissipation.

With the help of Water and Ethylene Glycol mixture as the base fluid and $Ag-TiO_2/WEG$ Casson hybrid nanoparticles Krishna et al.[20] analysed the flow of a MHD Casson hybrid nanofluid flow over an infinitely exponential accelerated vertical porous surface. An investigation of the unsteady MHD Al_2O_3, TiO_2 nanofluid flow over a moving vertical porous surface with a uniform transverse magnetic field and heat radiation, absorption effects has been done by Krishna et al.[21].

Based on the aforementioned research and its conceivable relevance to a number of scientific disciplines, it would be worthwhile to consider and investigate the aspects of higher order chemical reaction, Soret as well as Dufour effects on $Cu-H_2O$ nanofluid in a vertical plate contained in a porous medium concurrently with viscous dissipation, magnetic effects. Consideration is given to copper nanoparticles (Cu) due to their widespread use in food processing, water purification, and chemical processing (Dankovick and Smith[22]).

Many fluids used in industries will possess a uniform velocity acting along with it. Although a few researchers[2,7] have analyzed the fluid flow along with a constant velocity but such modeling in nanofluids is quite new. The originality of this work is in the numerical evaluation of a nanofluid travelling at a constant velocity through a vertical plate in porous media while being subjected to Dufour and Soret impacts in conjunction with a higher-order chemical reaction. We analyze the boundary layer equations by incorporating the nanoparticles and the base fluid's thermodynamical properties along with a uniform velocity. Through illustrations of the obtained graphs, we explore how each parameter affects velocity, temperature, and concentration. Using tables, we examine local skin friction coefficient, Nusselt number and Sherwood pertaining to fluid flow parameters.

Mathematical modeling

A vertical, semi-infinite plate contained in a porous medium is oriented along the x-axis. Envision a steady state nanofluid flow of a uniform velocity U_0 in the x-axis and the y-axis is normal to the x-axis as shown in Fig. 1. Nanofluid considered is incompressible, laminar and at steady state rotating along the y-axis with velocity Ω. A uniform magnetic field B_o is taken to be acting along the y-axis which is assumed to be electrically non conducting. We assume that the magnetic Reynolds number of the flow is taken to be small enough so that the induced magnetic field is negligible in comparison with applied one, so that the magnetic field acts along y-axis. Nanofluid provides an environment for chemical reactions of order n among species diffusing in it. Species concentrations near the wall and in the free stream significantly affect the flow. Because of this, we take into account the Dufour and Soret effects. Buoyancy is produced by a temperature disparity between the fluid and its surroundings. In this case, we take into account the buoyancy effects of both temperature and concentration. On the basis of aforementioned assumptions and the Boussinesq approximation, we can deduce these equations:

$$\frac{\partial u}{\partial x} + \frac{\partial v}{\partial y} = 0, \tag{1}$$

$$\rho_{nf}\left(u\frac{\partial u}{\partial x} + v\frac{\partial u}{\partial y}\right) = \mu_{nf}\left(\frac{\partial^2 u}{\partial y^2}\right) - \frac{\mu_{nf}}{K^*}(U_0 - u) + 2\Omega\rho_{nf}w + \sigma_{nf}B_o^2(U_0 - u) + (\rho\beta)_{nf}g(T - T_\infty) + (\rho\beta)_{nf}g(C - C_\infty), \tag{2}$$

$$\rho_{nf}(u\frac{\partial w}{\partial x} + v\frac{\partial w}{\partial y}) = \mu_{nf}(\frac{\partial^2 w}{\partial y^2}) - \frac{\mu_{nf}}{K^*}w + 2\Omega\rho_{nf}(U_0 - u) - \sigma_{nf}B_o^2 w, \tag{3}$$

$$u\frac{\partial T}{\partial x} + v\frac{\partial T}{\partial y} = \frac{\kappa_{nf}}{(\rho C_p)_{nf}}\frac{\partial^2 T}{\partial y^2} + \frac{D_m K_T}{C_s C_p}\frac{\partial^2 C}{\partial y^2} + \frac{\mu_{nf}}{(\rho C_p)_{nf}}[(\frac{\partial u}{\partial x})^2 + (\frac{\partial w}{\partial y})^2] + \frac{\sigma_{nf}B_o^2}{(\rho C_p)_{nf}}[(U_0 - u)^2 + w^2], \tag{4}$$

$$u\frac{\partial C}{\partial x} + v\frac{\partial C}{\partial y} = D_m\frac{\partial^2 C}{\partial y^2} + \frac{D_m K_T}{T_m}\frac{\partial^2 T}{\partial y^2} - k_r(C - C_\infty)^n. \tag{5}$$

With boundary conditions,

$$\begin{aligned} u = 0, v = v_0(x), w = 0, T = T_w, C = C_w \quad \text{at} \quad y = 0 \\ u \to U_0, w \to 0, T \to T_\infty, C \to C_\infty \quad \text{as} \quad y \to \infty. \end{aligned} \tag{6}$$

Here, u, v, w are velocities in x, y, z directions. B_0 is applied magnetic field, C_p is specific heat at constant pressure, C_s is concentration susceptibility, C is nanofluid's local concentration, C_w is nanofluid's concentration on wall, C_∞ is nanofluid's concentration in free stream, D_m is molecular diffusivity, g denotes acceleration due to gravity, K^* denotes permeability parameter, K_T denotes thermal diffusivity ratio, k_r denotes chemical reaction parameter, n is chemical reaction's order, T is nanofluid's local temperature, T_w is nanofluid's temperature on the wall, T_∞ is nanofluid's temperature in free stream, T_m is mean fluid temperature.

We now have two velocities U_0 (a constant velocity acting along with the fluid) and u (velocity along the x-axis). For the ease of solving the problem, we define a velocity u_1, $u_1 = U_0 - u$ as per the idea used by Raptis and Pfrdikis[23].

As a consequence of applying the transformation $u_1 = U_0 - u$, the Eqs. (1 to 5) and the boundary condition (6) are transformed into the following equations.

$$-\frac{\partial u_1}{\partial x} + \frac{\partial v}{\partial y} = 0, \tag{7}$$

$$\rho_{nf}((U_0 - u_1)\frac{\partial u_1}{\partial x} + v\frac{\partial u_1}{\partial y}) = \mu_{nf}(\frac{\partial^2 u_1}{\partial y^2}) - \frac{\mu_{nf}}{K^*}u_1 - 2\Omega\rho_{nf}w - \sigma_{nf}B_o^2 u_1 - (\rho\beta)_{nf}g(T - T_\infty) - (\rho\beta)_{nf}g(C - C_\infty), \tag{8}$$

$$\rho_{nf}((U_0 - u_1)\frac{\partial w}{\partial x} + v\frac{\partial w}{\partial y}) = \mu_{nf}(\frac{\partial^2 w}{\partial y^2}) - \frac{\mu_{nf}}{K^*}w + 2\Omega\rho_{nf}u_1 - \sigma_{nf}B_o^2 w, \tag{9}$$

$$(U_0 - u_1)\frac{\partial T}{\partial x} + v\frac{\partial T}{\partial y} = \frac{\kappa_{nf}}{(\rho C_p)_{nf}}\frac{\partial^2 T}{\partial y^2} + \frac{D_m K_T}{C_s C_p}\frac{\partial^2 C}{\partial y^2} + \frac{\mu_{nf}}{(\rho C_p)_{nf}}[(\frac{\partial u_1}{\partial x})^2 + (\frac{\partial w}{\partial y})^2] + \frac{\sigma_{nf}B_o^2}{(\rho C_p)_{nf}}[(u_1)^2 + w^2], \tag{10}$$

$$(U_0 - u_1)\frac{\partial C}{\partial x} + v\frac{\partial C}{\partial y} = D_m\frac{\partial^2 C}{\partial y^2} + \frac{D_m K_T}{T_m}\frac{\partial^2 T}{\partial y^2} - k_r(C - C_\infty)^n. \tag{11}$$

The boundary conditions are

$$\begin{aligned} u_1 = U_0, v = v_0(x), w = 0, T = T_w, C = C_w \quad \text{at} \quad y = 0 \\ u_1 \to 0, w \to 0, T \to T_\infty, C \to C_\infty \quad \text{as} \quad y \to \infty. \end{aligned} \tag{12}$$

Thermodynamical properties of nanofluids are

$$\begin{aligned} \mu_{nf} = \frac{\mu_f}{(1-\phi_0)^{2.5}}, v_{nf} = \frac{\mu_{nf}}{\rho_{nf}}, \rho_{nf} = (1-\phi_0)\rho_f + \phi_0\rho_s, (\rho\beta)_{nf} = (1-\phi_0)(\rho\beta)_f + \phi_0(\rho\beta)_s, \\ (\rho C_p)_{nf} = (1-\phi_0)(\rho C_p)_f + \phi_0(\rho C_p)_s, \kappa_{nf} = \frac{(\kappa_s + 2\kappa_f) - 2\phi_0(\kappa_f - \kappa_s)}{(\kappa_s + 2\kappa_f) + 2\phi_0(\kappa_f - \kappa_s)}. \end{aligned} \tag{13}$$

Here, β_f is base fluid's thermal expansion coefficient, β_{nf} is nanofluid's thermal expansion coefficient, β_s is nanoparticle's thermal expansion coefficient, ρ_f is base fluid's density, ρ_s is nanoparticle's density, ρ_{nf} is nanofluid's density, $(\rho C_p)_{nf}$ is nanofluid's heat capacitance, μ_f is base fluid's dynamic viscosity, μ_s is nanoparticle's dynamic viscosity, μ_{nf} is nanofluid's dynamic viscosity, v_f is base fluid's kinematic viscosity, v_s is kinematic viscosity of nanoparticles, σ_{nf} is nanofluid's electrical conductivity, v_{nf} is nanofluid's kinematic viscosity, ϕ_0 is nanofluid's volume fraction, κ_{nf} is nanofluid's conductivity, $(C_p)_{nf}$ is nanofluid's specific heat.

The Eqs. (7)–(11) serve as the basic governing equations here. Utilizing transformations (14), the governing Eqs. (7)–(11), as well as the boundary conditions (12) are solved.

$$\eta = y\sqrt{\frac{U_0}{2\nu x}}, g(\eta) = \frac{w}{U_0}, \theta = \frac{T - T_\infty}{T_w - T\infty}, \phi = \frac{C - C_\infty}{C_w - C_\infty}, \psi = \sqrt{2\nu x U_0} f(\eta),$$

$$u_1 = \frac{\partial \psi}{\partial y} = U_0 f'(\eta) \Rightarrow \frac{u}{U_0} = 1 - f'(\eta), f_w = v_0(x)\sqrt{\frac{2x}{U_0 \nu}}. \tag{14}$$

By substituting (13) and (14) in Eqs. (7)–(11),

$$v = -\sqrt{\frac{U_0 \nu}{2x}}(\eta f' - f), \tag{15}$$

$$f''' = \frac{1}{a_1}[-f''(\eta - f) + \frac{a_1 f'}{K} + Rg + \frac{Mf'}{a_2} + \frac{a_3}{a_2} Ri(\theta + N\phi)], \tag{16}$$

$$g'' = \frac{1}{a_1}[-g'(\eta - f) + \frac{a_1 g}{K} - Rf' + a_4 Mg], \tag{17}$$

$$\theta'' = \frac{1}{a_5 - a_6 PrScSoDu}[a_6(\eta - f)(DuScPr\phi' - \theta') - MEcPr[(f')^2 + g^2] - a_6 a_7 PrEc[(f'')^2 + (g')^2] + a_6 PrDuSc\gamma\phi^n], \tag{18}$$

$$\phi'' = \frac{1}{a_5 - a_6 PrScSoDu}[Sc(\eta - f)(a_6 SoPr\theta' - a_5\phi') - MEcPrScSo[(f')^2 + g^2]$$
$$- a_6 a_7 PrEcScSo[(f'')^2 + (g')^2] + a_5 Sc\gamma\phi^n]. \tag{19}$$

The associated boundary conditions are

$$f = f_w, f' = 1, g = 0, \theta = 1, \phi = 1 \quad \text{at} \quad \eta = 0$$
$$f' \to 0, g \to 0, \theta \to 0, \phi \to 0 \quad \text{as} \quad \eta \to \infty, \tag{20}$$

where primes refer to derivatives about η; Here

$$M = \frac{2\sigma_{nf}B_0^2 x}{U_0 \rho_f}, K = \frac{2\nu_f x}{K^* U_0}, Ri = \frac{(\nu_f)^2 g\beta_f(T_w - T_\infty)}{x(U_0)^2}, N = \frac{T_w - T_\infty}{C_w - C_\infty}, Re_x = \frac{xU_0}{\nu},$$

$$R = \frac{4x\Omega}{U_0}, Pr = \frac{(\mu C_p)_f}{K_f}, Du = \frac{D_m K_t}{C_s C_p \nu_f}\frac{C_w - C_\infty}{T_w - T_\infty}, \gamma = \frac{2k_r x}{U_0}(C_w - C_\infty)^{n-1},$$

$$Sc = \frac{\nu_f}{D_m}, So = \frac{D_m K_t}{\nu_f T_m}\frac{T_w - T\infty}{C_w - C_\infty}, Ec = \frac{U_0^2}{C_p(T_w - T_\infty)}, a_1 = \frac{1}{(1 - \phi_0)^{2.5}}\frac{1}{(1 - \phi_0) + \phi_0(\frac{\rho_s}{\rho_f})},$$

$$a_2 = (1 - \phi_0) + \phi_0(\frac{\rho_s}{\rho_f}), a_3 = (1 - \phi_0) + \phi_0(\frac{(\rho\beta)_s}{(\rho\beta)_f}),$$

$$a_4 = \frac{1}{(1 - \phi_0) + \phi_0(\frac{\rho_s}{\rho_f})}, a_5 = \frac{(\kappa_s + \kappa_f) - 2\phi_0(\kappa_f - \kappa_s)}{(\kappa_s + \kappa_f) + 2\phi_0(\kappa_f + \kappa_s)}\cdot\frac{1}{\kappa_f},$$

$$a_6 = ((1 - \phi_0)(\rho C_p)_f + \phi_0(\rho C_p)_s), a_7 = \frac{(1 - \phi_0)^{2.5}}{((1 - \phi_0)(\rho C_p)_f + \phi_0(\rho C_p)_s)}. \tag{21}$$

In the above quantities, T_w denotes temperature on wall and C_w is concentration on wall; θ and ϕ are dimensionless temperature and dimensionless concentration; Ec is Eckert number; M symbolizes dimensionless magnetic field parameter; K is dimensionless permeability parameter; γ symbolizes dimensionless chemical reaction parameter; Re_x is Reynolds number; R is rotation parameter; Ri symbolizes Richardson number; Pr symbolizes Prandtl number; Sc symbolizes Schmidt number; Du and So symbolize Dufour and Soret effects. For practical applications, local skin friction coefficient, Nusselt number, Sherwood number are relevant physical quantities, that are defined as:

Local Skin friction coefficient, $Cf_x = \frac{\tau_w}{\rho_f v_0^2} \Rightarrow \sqrt{2}Cf_x(1 - \phi_0)^{2.5} = f''(0)$.

Local Nusselt number, $Nu_x = \frac{xq_w}{K_f(T_w - T_\infty)} \Rightarrow \sqrt{2}\frac{Nu_x}{Re_x}\frac{K_f}{K_{nf}} = -\theta'(0)$.

Local Sherwood number, $Sh_x = \frac{xq_m}{D_B(C_w - C_\infty)} \Rightarrow \sqrt{2}\frac{Sh_x}{Re_x} = -\phi'(0)$.

where $\tau_w = \mu_{nf}(\frac{\partial u}{\partial y})_{y=0}$, is the wall shear stress, $q_w = -K_{nf}(\frac{\partial T}{\partial y})_{y=0}$, is the wall heat flux, $q_m = -D_B(\frac{\partial C}{\partial y})_{y=0}$, is the wall mass flux.

Thermodynamical properties	H_2O	Cu
C_p (J/(kg K))	4179	385
ρ (kg/m^3)	997.1	8933
κ (W/m K)	0.613	400
$\beta \times 10^{-5}$ (K^{-1})	21	1.67

Table 1. Thermodynamical properties of nanofluids (Oztop et al.[24]).

Method of solution

In order to solve Eqs. (16)–(20) using the bvp4c package in MATLAB, the construction of functions that give solutions to differential equations with boundary conditions is necessary. Consider, $f = f(1); f' = f(2); f'' = f(3); g = f(4); g' = f(5); \theta = f(6); \theta' = f(7); \phi = f(8); \phi' = f(9);$

Eqs. (16)–(19) are transformed into the following first order differential equations.

$$\begin{bmatrix} f' \\ f'' \\ f''' \\ g' \\ g'' \\ \theta' \\ \theta'' \\ \phi' \\ \phi'' \end{bmatrix} = \begin{bmatrix} f(2) \\ f(3) \\ \frac{1}{a_1}((f(1)f(3)) + (\frac{a_1 f(2)}{K}) + (\frac{M}{a_2}f(2)) - (\eta f(3)) + (Rf(4)) + (\frac{a_3}{a_2}Ri((f(6))) + Nf(8))) \\ f(5) \\ \frac{1}{a_1}((f(1)f(4)) - (Rf(2)) + (\frac{a_1 f(4)}{K}) + (a_4 Mf(4)) - (\eta f(4)) \\ f(7) \\ \frac{1}{a_5 - a_6 PrScSoDu}[a_6(\eta - f(1))(DuScPrf(9) - f(7)) - MEcPr[(f(2))^2 + (f(4))^2] - a_6 a_7 PrEc[(f(3))^2 + (f(5))^2] + a_6 PrDuSc\gamma (f(8))^n] \\ f(9) \\ \frac{1}{a_5 - a_6 PrScSoDu}[Sc(\eta - f(1))(a_6 Soprf(7) - f(9)) - MEcPrScSo[(f(2))^2 + (f(4))^2] - a_6 a_7 PrEcScSo[(f(3))^2 + (f(5))^2] + a_5 Sc\gamma (f(8))^n]. \end{bmatrix}$$

When this problem is viewed as an initial value problem, a numerical solution can be found. MATLAB's bvp4c package has been used to solve these equations.

Results and discussion

Specifically, the intention of this work is to analyze how a rotating nanofluid with a constant velocity interacts with a higher order chemical reaction through a plate in conjunction with a porous medium, viscous dissipation and a magnetic field. Keeping in mind, the real-life applications of the order of chemical reaction, the value of n is restricted to 3, and a comparison is provided in the following figures for $n = 1$ and $n = 3$. Additionally, the influence of M, Ri, Du, So, Ec, γ on the velocity of the flow, temperature, and concentration of the nanofluid-Cu$-$H$_2$O are presented by graphs in the Figs. 2, 3, 4, 5, 6, 7, 8, 9, 10, 11, 12 and 13. The nanofluid is formed by suspending copper nanoparticles in water with a volume fraction of 0.15. This problem is solved while considering the thermodynamic properties of both Cu and H$_2$O. The thermodynamical properties of Cu and H$_2$O are given in Table 1.

In this paper, for the Figs. 2, 3, 4, 5, 6, 7, 8, 9, 10, 11, 12 and 13, we have used $Ri = 4$; $R = 2$; $K = 2$; $Pr = 6.785$; $Du = 3$; $Sc = 0.6$; $\gamma = 2$; $f_w = 0.5$; $Ec = 1$; $So = 1$; $N = 1$;

Variable parameters are mentioned against the respective graphs.

Figure 2 depicts the velocity for different Ri and n. For increasing Ri, there is an increase in buoyancy due to which the fluid velocity increases. An increase in n increases the velocity as well. Figure 3 represents the velocity profile for increasing n and K. A lower value of n results in a lower velocity profile. The velocity increases with an increase in K for a given n value. Since the ability of the fluid to penetrate into the medium increases with increasing permeability parameter, fluid velocity increases.

The velocity profile in Fig. 4 is illustrated for a variety of M and n values. It is evident that velocity decreases as n increases. Velocity falls when M increases for a specific value of n. The Lorentz force begins to take control when M increases, thus lowering the velocity. Figure 5 represents concentration profile for different M and n. A higher n value results in higher concentration. The concentration increases with an increase in M for a given n.

A velocity profile can be observed in Fig. 6 for various values of Du and n. The increase in velocity is proportionate to Du. The velocity is not affected by an increase in Du when n is low. As n rises, the flow velocity increases at higher Du. At high Du and high n, the flow velocity is maximum. It is illustrated in Fig. 7 how the temperature changes as Du and n increase. Increasing n seems to increase the temperature of the system when Du is higher. If Du is lower, increasing n does not increase the velocity of the system. An enhancement in Du increases the molecular collisions from hotter to colder regions, which enhances the temperature.

Figures 8 and 9 reveal velocity and concentration profile for different So, n. For a particular value of n, an increase in So increases velocity as well as concentration. This is because of the influence of thermal gradients on the diffusing species. Increasing n rises the velocity profile and the concentration profile.

Kinesis and heat are measured by Eckert number (viscous dissipation parameter). In the presence of viscous fluid stresses, kinetic energy is changed into internal energy. Higher Ec indicates high kinetic energy resulting in increased fluid vibrations and larger collisions between molecules. The boundary layer region becomes hotter as the amount of molecule collisions increases, dissipating more heat. A more rapid flow and higher temperature are therefore associated with a rise in viscous dissipation parameter. With an increase in n, collisions will increase, resulting in higher velocity and temperature. Figures 10 and 11 illustrate these trends.

Figures 12 and 13 depict velocity and concentration profiles for increasing values of γ and n. An increase in γ translates into a rise in the number of molecules of solute going through chemical reactions, leading to a
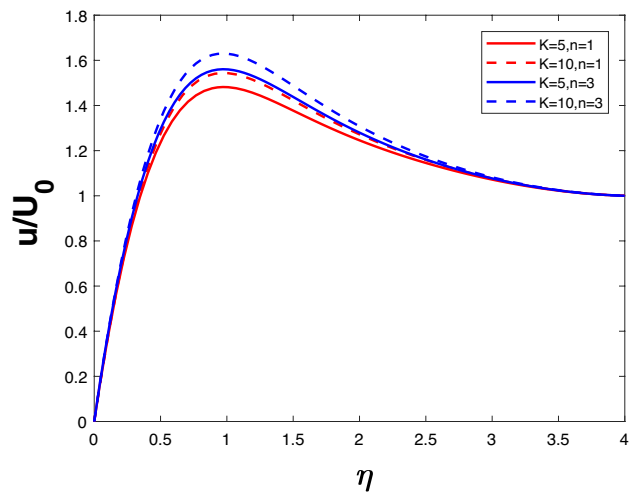
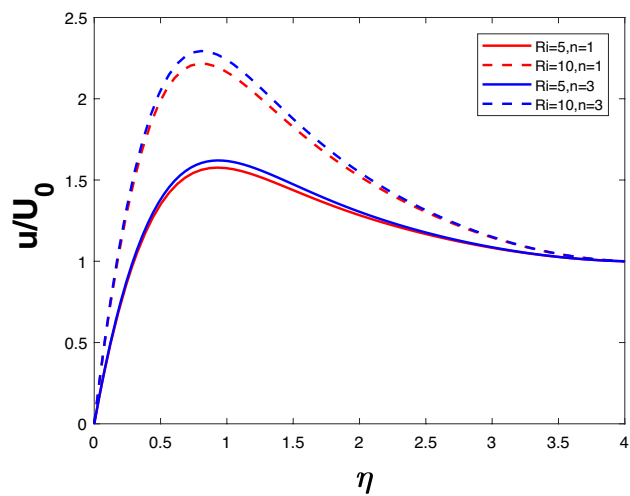**Figure 2.** Velocity profile for various *K*.
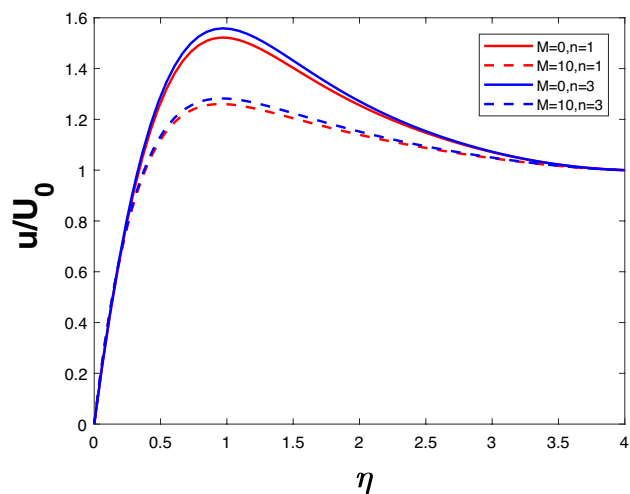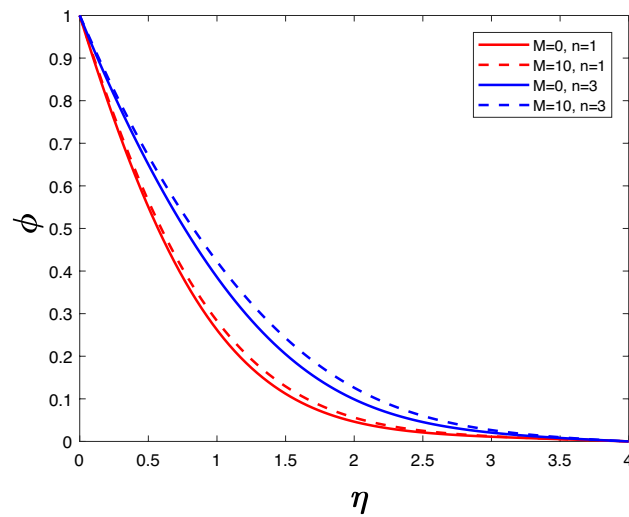

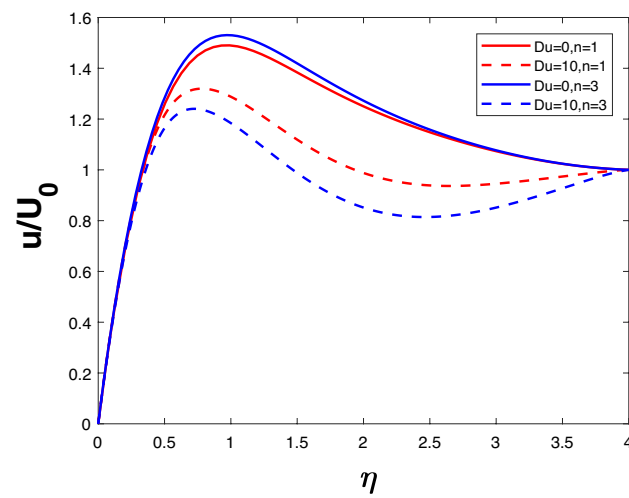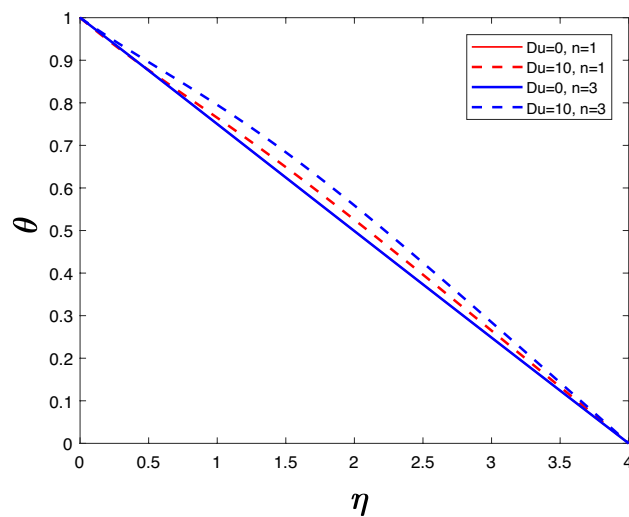**Figure 3.** Velocity profile for various *Ri*.
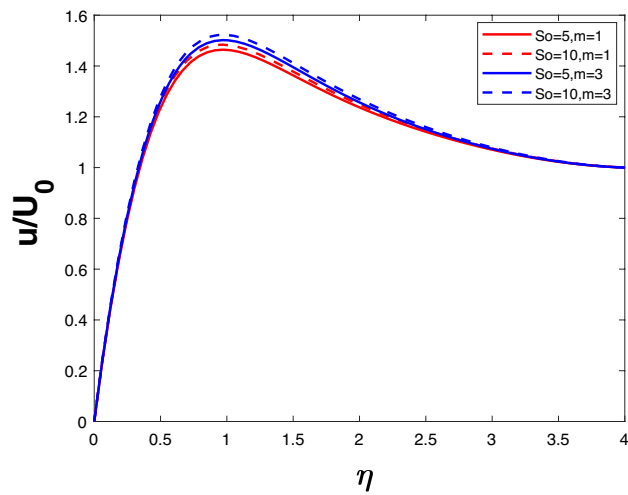

Figure 4. Velocity profile for various *M*.
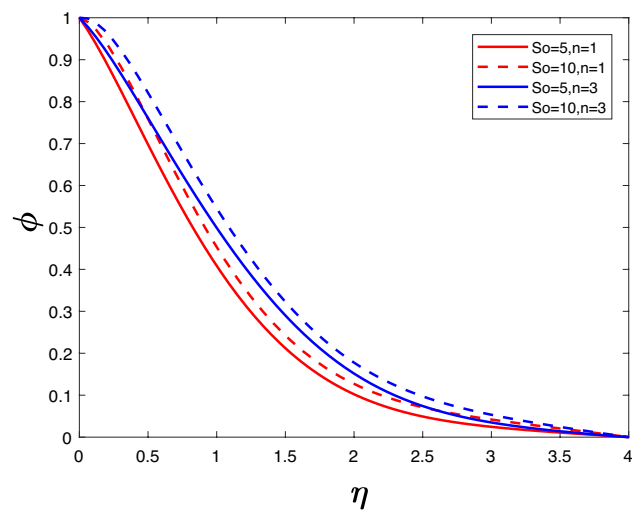
Figure 5. Concentration profile for various *M*.

Figure 6. Velocity profile for various *Du*.

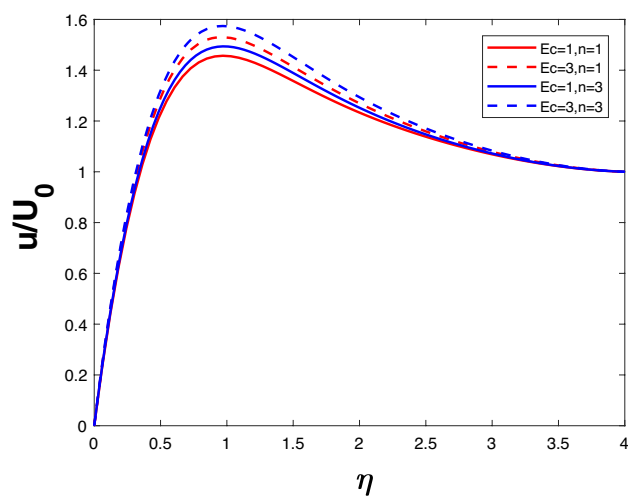**Figure 7.** Temperature profile for various *Du*.

Figure 8. Velocity profile for various *So*.

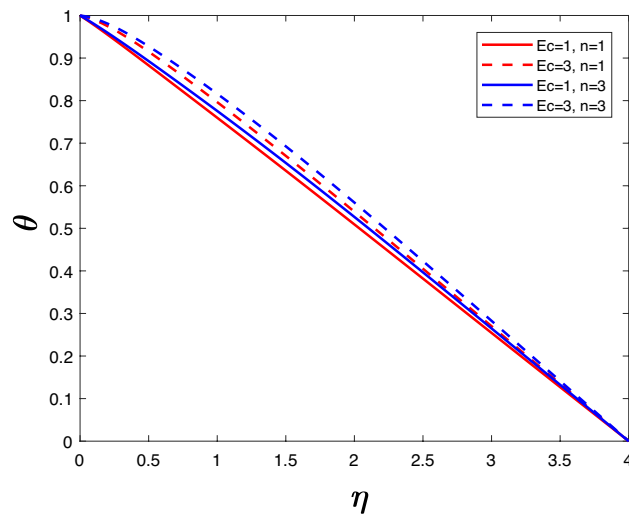
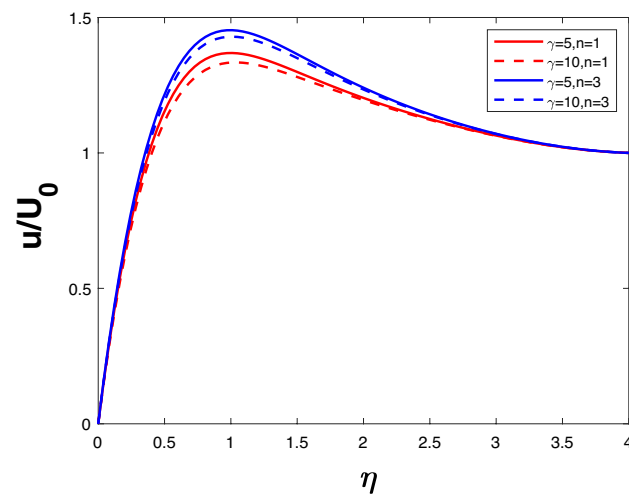**Figure 9.** Concentration profile for various *So*.
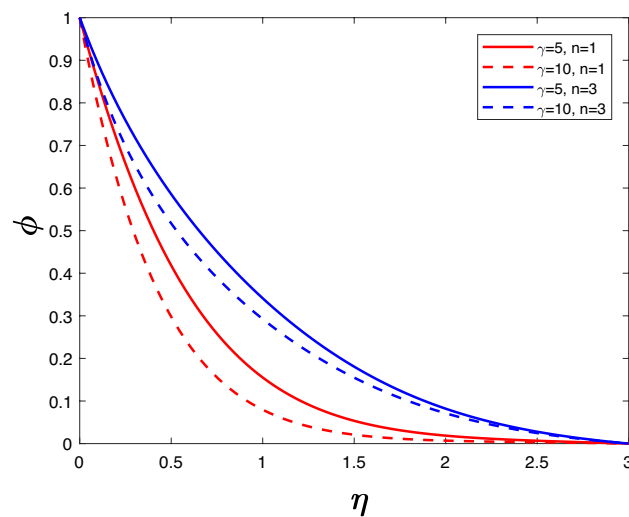

Figure 10. Velocity profile for various *Ec*.

Figure 11. Temperature profile for various *Ec*.

Figure 12. Velocity profile for various γ.

Figure 13. Concentration profile for various γ.

	Alam et al.[7]	Present results
Ec	$f''(0)$	$f''(0)$
0.01	− 3.691740	− 3.686071
0.05	− 3.721830	− 3.719738
0.10	− 3.761275	− 3.763524
0.15	− 3.802958	− 3.809364
0.20	− 3.847133	− 3.857470
0.25	− 3.894094	− 3.908065

Table 2. Comparison of present results with Alam et al.[7] with $Ri = 4; N = 0.5; R = 0.2; K = 0.5;$ $M = 0.5; Pr = 0.71; Du = 0.2; Sc = 0.6; \gamma = 0; Ec = 0.01; So = 0.2; \phi_0 = 0.$

Du	n	$f''(0)$	$-\theta'(0)$	$-\phi(0)$
1	1	− 2.308111	0.216378	0.841627
	2	− 2.355917	0.218110	0.924221
	3	− 2.378565	0.221718	1.079250
2	1	− 2.307127	0.217289	0.842691
	2	− 2.355410	0.220057	0.924967
	3	− 2.378237	0.225729	1.079490
3	1	− 2.306160	0.218143	0.843773
	2	− 2.354914	0.221948	0.925727
	3	− 2.377922	0.229694	1.079731
4	1	− 2.305205	0.218937	0.844875
	2	− 2.354429	0.223782	0.926501
	3	− 2.377616	0.233613	1.079975

Table 3. Variation of local skin friction coefficient, Nusselt number, Sherwood number for various values of Du for $n = 1, 2, 3$.

So	n	$f''(0)$	$-\theta'(0)$	$-\phi(0)$
1	1	− 2.380070	0.217950	0.827176
	2	− 2.356993	0.221777	0.909210
	3	− 2.305027	0.229576	1.063647
2	1	− 2.377922	0.218143	0.843773
	2	− 2.354914	0.221948	0.925727
	3	− 2.306160	0.229694	1.079731
3	1	− 2.375789	0.218329	0.860279
	2	− 2.352849	0.222114	0.942146
	3	− 2.304310	0.229808	1.095714
4	1	− 2.373669	0.218510	0.876697
	2	− 2.350800	0.222274	0.958470
	3	− 2.302476	0.229918	1.111599

Table 4. Variation of local skin friction coefficient, Nusselt number, Sherwood number for various values of So for $n = 1, 2, 3$.

reduction in velocity and concentration. Increasing n rises the velocity profile and the concentration profile despite the opposing effects of the chemical reaction parameter.

Table 2 provides a limiting case comparison of our results with the results of Alam et al.[7] with $Ri = 4; N = 0.5; R = 0.2; K = 0.5; M = 0.5; Pr = 0.71; Du = 0.2; Sc = 0.6; \gamma = 0; Ec = 0.01; So = 0.2; \phi_0 = 0.$ Our results are in good agreement with the existing literature. Tables 3 and 4 shows values of $f''(0), -\theta'(0), -\phi'(0)$ for increasing Du, So when $n = 1, 2, 3$. As seen, as Du increases, it increases $-\phi'(0)$ and as So increases $-\theta'(0)$ also increase because of Thermo-diffusion and Diffusion-thermo effects created in the fluid.

Conclusion

A comprehensive investigation is performed with a focus on the influences of higher order chemical reaction, magnetic parameter, permeability parameter, viscous dissipation, Dufour and Soret effects on $Cu-H_2O$ nanofluid through a vertical plate. The $Cu-H_2O$ nanofluid is considered to flow through a constant velocity acting along with it. This investigation leads us to the following conclusions.

- Heat and mass transfer are more rapid in higher order chemical reaction than in low order reaction.
- Increasing the values of magnetic parameter M, chemical reaction parameter γ opposes the nanofluid flow while an increase in Dufour number Du, permeability paramter K, Eckert number Ec aids to the flow of the nanofluid.
- The temperature of the nanofluid rises as the heat in boundary layer rises due to a rise in Dufour number Du and Eckert number Ec.
- The concentration of nanofluid boosts up with an increase in Soret number So while an opposite trend is observed for increasing values of chemical reaction paramter γ.
- For a particular order of a chemical reaction, the rate of heat transfer increases for increasing Soret number So while an enhancement in Dufour number Du enhances the mass transfer rate.

Moreover, the results of this investigation can be applied to industries manufacturing chemicals such as fertilizers, polymers, and color dyes on a large scale where the faster rates of chemical reactions are significant.

Data availability

The datasets used and/or analysed during the current study available from the corresponding author on reasonable request.

References

1. Rahman, M. & Al-Lawatia, M. Effects of higher order chemical reaction on micropolar fluid flow on a power law permeable stretched sheet with variable concentration in a porous medium. *The Canadian Journal of Chemical Engineering* **88**(1), 23–32 (2010).
2. Mallikarjuna, B., Bhuvanavijaya, R.: Effect of higher order chemical reaction on mhd non-darcy convective heat and mass transfer over a vertical plate in a rotating system embedded in a fluid saturated porous medium with non-uniform heat source/sink. In: Proceedings of the 22th National and 11th International ISHMTASME Heat and Mass Transfer Conference. pp. 28-31 (2013).
3. Rajani, D., Hemalatha, K.: Effects of higher order chemical reactions and slip boundary conditions on nano fluid flow. Int. J. of Eng. Res. and Application **7**(5),36-45 (2017).
4. Matta, A. & Gajjela, N. Order of chemical reaction and convective boundary condition effects on micropolar fluid flow over a stretching sheet. *AIP advances* **8**(11), 115212 (2018).
5. Sastry, R.: Melting and radiation effects on mixed convection boundary layer viscous flow over a vertical plate in presence of homogeneous higher order chemical reaction. Frontiers in Heat and Mass Transfer (FHMT) 11 (2018).
6. Chen, C.H.: Combined effects of joule heating and viscous dissipation on magneto-hydrodynamic flow past a permeable, stretching surface with free convection and radiative heat transfer. Journal of Heat Transfer **132**(6) (2010)
7. Alam, M. M., Hossain, M. D. & Hossain, M. A. Viscous dissipation and joule heating effects on steady mhd combined heat and mass transfer flow through a porous medium in a rotating system. *Journal of Naval Architecture and Marine Engineering* **8**(2), 105–120 (2011).
8. Jaber, K. K. *et al.* Joule heating and viscous dissipation on effects on mhd flow over a stretching porous sheet subjected to power law heat flux in presence of heat source. *Open Journal of fluid dynamics* **6**(03), 156 (2016).
9. Pandey, A. K. & Kumar, M. Effect of viscous dissipation and suction/injection on mhd nano fluid flow over a wedge with porous medium and slip. *Alexandria Engineering Journal* **55**(4), 3115–3123 (2016).
10. Prakash, D., Suriyakumar, P., Sivakumar, N. & Kumar, B. R. Influence of viscous and ohmic heating on mhd flow of nanofluid over an inclined nonlinear stretching sheet embedded in a porous medium. *International Journal of Mechanical Engineering and Technology (IJMET)* **9**(8), 992–1001 (2018).
11. Reddy, N. N., Rao, V. S. & Reddy, B. R. Chemical reaction impact on mhd natural convection flow through porous medium past an exponentially stretching sheet in presence of heat source/sink and viscous dissipation. *Case Studies in Thermal Engineering* **25**, 100879 (2021).
12. Choi, S., Eastman, J.: Enhancing thermal conductivity of fluids with nanoparticles. Proceedings of the ASME International Mechanical Engineering Congress and Exposition **66** (1995)
13. Sheikholeslami, M. & Ebrahimpour, Z. Thermal improvement of linear Fresnel solar system utilizing Al_2O_3-water nanofluid and multi-way twisted tape. *International Journal of Thermal Sciences* **176**, 107505 (2022).
14. Sheikholeslami, M. Numerical analysis of solar energy storage within a double pipe utilizing nanoparticles for expedition of melting. *Solar Energy Materials and Solar Cells* **245**, 111856 (2022).
15. Sheikholeslami, M. & Ebrahimpour, Z. Nanofluid performance in a solar LFR system involving turbulator applying numerical simulation. *Advanced Powder Technology* **33**(8), 103669 (2022).
16. Jagadha, S., Gopal, D., Kishan, N.: Nanofluid flow of higher order radiative chemical reaction with effects of melting and viscous dissipation. In: Journal of Physics:Conference Series. vol. 1451. IOP Publishing (2020)
17. Swain, B. K., Parida, B. C., Kar, S. & Senapati, N. Viscous dissipation and joule heating effect on MHD flow and heat transfer past a stretching sheet embedded in a porous medium. *Heliyon* **6**(10), e05338 (2020).
18. Alaidrous, A. A. & Eid, M. R. 3-d electromagnetic radiative non-newtonian nanofluid flow with joule heating and higher-order reactions in porous materials. *Scientific Reports* **10**(1), 1–19 (2020).
19. Gopal, D. *et al.* Numerical analysis of higher order chemical reaction on electrically mhd nanofluid under influence of viscous dissipation. *Alexandria Engineering Journal* **60**(1), 1861–1871 (2021).
20. Krishna, M. V., Ahammad, N. A. & Chamkha, A. J. Radiative MHD flow of Casson hybrid nanofluid over an infinite exponentially accelerated vertical porous surface. *Case Studies in Thermal Engineering* **27**, 101229 (2021).
21. Krishna, M. V., Ahamad, N. A. & Chamkha, A. J. Radiation absorption on MHD convective flow of nanofluids through vertically travelling absorbent plate. *Ain Shams Engineering Journal* **12**(3), 3043–3056 (2021).

11

22. Dankovich, T. A. & Smith, J. A. Incorporation of copper nanoparticles into paper for point-of-use water purification. *Water research* **63**, 245–251 (2014).
23. Raptis, A. & Pfrdikis, C. Combined free and forced convection flow through a porous medium. *International Journal of Energy Research* **12**(3), 557–560 (1988).
24. Oztop, Hakan F., and Eiyad Abu-Nada.: Numerical study of natural convection in partially heated rectangular enclosures filled with nanofluids. International journal of heat and fluid flow **29** (5), 1326-1336 (2008)

Author contributions

Conception and design of the study done by Dr. R.K.B. and P.K. wrote the main manuscript text and prepared figures and Tables. Both the authors reviewed and finalized the manuscript.

Competing interests

The authors declare no competing interests.

Additional information

Correspondence and requests for materials should be addressed to R.K.B.

Reprints and permissions information is available at www.nature.com/reprints.

Publisher's note Springer Nature remains neutral with regard to jurisdictional claims in published maps and institutional affiliations.